Electronic Supplementary Material (ESI) for Nanoscale.

Supporting Information for

Bias-tunable two-dimensional magnetic and topological materials

Jie Li and Ruqian Wu*

Department of Physics and Astronomy, University of California, Irvine, California 92697-4575, USA.

* E-mail: wur@uci.edu

The detail of torque method

In the Torque method, the torque *T(θ)* as a function of the polar angle θ between the magnetization and the z is defined as,

$$T(\theta) = \frac{dE(\theta)}{d\theta} = \sum_{occ} \left\langle \psi_{ik} \left| \frac{\partial H_{so}}{\partial \theta} \right| \psi_{ik} \right\rangle \quad (1)$$

with the spin-orbit coupling (SOC) Hamiltonian $H_{so} = \sum_i \xi(r_i)\hat{l}_i \cdot \hat{s}$, and the summation goes over all occupied states. By integrating *T(θ)*, we obtain the total energy $E(\theta)$ as a function of the polar angle θ, and the MAE is equal to the difference between the lowest and highest total energies.

	Ti	V	Cr	Mn	Fe	Co	Ni	Cu	Zn
$M@C_u$	1.579	1.462	1.635	2.245	2.308	2.185	2.485	2.46	2.179
$M@C_d$	1.717	1.528	2.025	2.117	2.706	1.704	2.401		
$M@H_{1\text{-}u}$	0.87	1.272	1.516	2.494	1.883	2.369	2.567	2.97	2.71
$M@H_{1\text{-}d}$	0.27	1.017	1.729	2.495	2.12	2.454	3.079		
$M@H_{2\text{-}u}$	0.616	1.229	1.452	2.33	1.7	2.311	2.439	2.835	2.55
$M@H_{2\text{-}d}$	0.345	0.715	1.501	2.331	1.993	2.263	2.991		

Table S1. The binding energies (eV) of M@C, $M@H_1$ and $M@H_2$ (M= Ti - Zn).

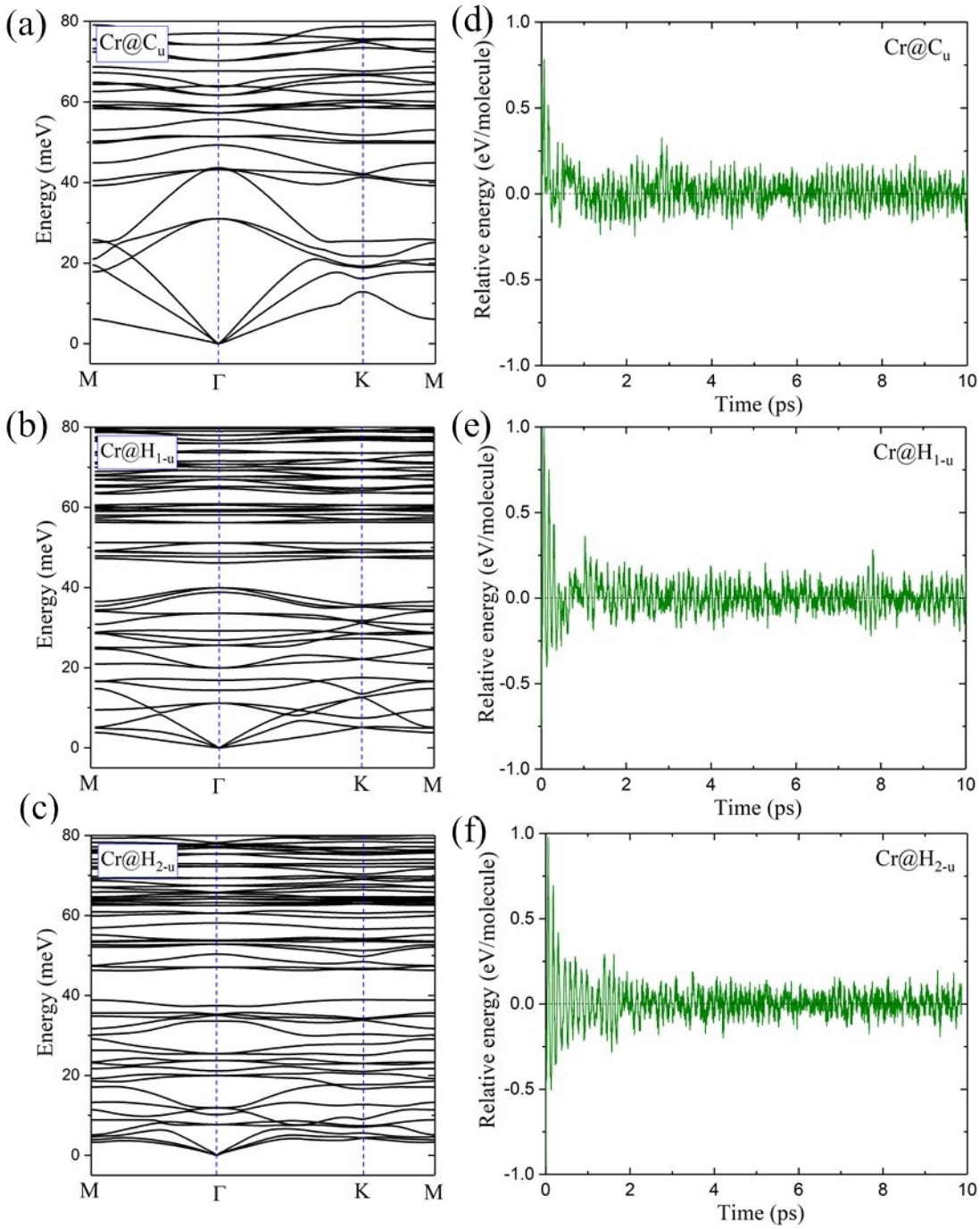

Fig. S1 The phonon spectrum and the relative total energy as function of AIMD time for Cr@C_u, Cr@H_{1-u} and Cr@H_{2-u}, respectively. (a), (d) for Cr@C_u, (b), (e) for Cr@H_{1-u}, (c), (f) for Cr@H_{2-u}.

Table S2. The atomic displacements (Δd, in Å) of M@C, M@H_1 and M@H_2 (M= Ti-Ni).

	Ti	V	Cr	Mn	Fe	Co	Ni
M@C	0.02	0.03	0.001	0.01	0.001	0.49	0.82
M@H_1	0.775	1.09	1.22	0.001	0.74	0.97	0.82
M@H_2	0.40	1.08	0.40	0.001	0.33	0.94	0.77

Table S3. The height (h, in Å) of the carbon cage in different lattices.

	Ti	V	Cr	Mn	Fe	Co	Ni
$M@C_u$	4.31	4.32	4.30	4.31	4.27	4.37	4.35
$M@C_d$	4.33	4.33	4.31	4.30	4.27	4.39	4.37
$M@H_{1\text{-}u}$	4.52	4.57	4.56	4.55	4.52	4.56	4.61
$M@H_{1\text{-}d}$	4.54	4.56	4.55	4.55	4.54	4.53	4.53
$M@H_{2\text{-}u}$	4.50	4.54	4.58	4.54	4.53	4.56	4.60
$M@H_{2\text{-}d}$	4.53	4.56	4.53	4.54	4.54	4.50	4.47

Table S4. The energy barriers (eV) between phase I nad II of M@C, M@H_1 and M@H_2 (M= Ti-Ni).

	Ti	V	Cr	Mn	Fe	Co	Ni
M@C	0.077	0.041	0.010	0.163	0.001	0.559	0.306
M@H_1	1.000	0.449	0.211	0.001	0.205	0.161	0.450
M@H_2	0.597	0.779	0.423	0.001	0.186	0.011	0.501

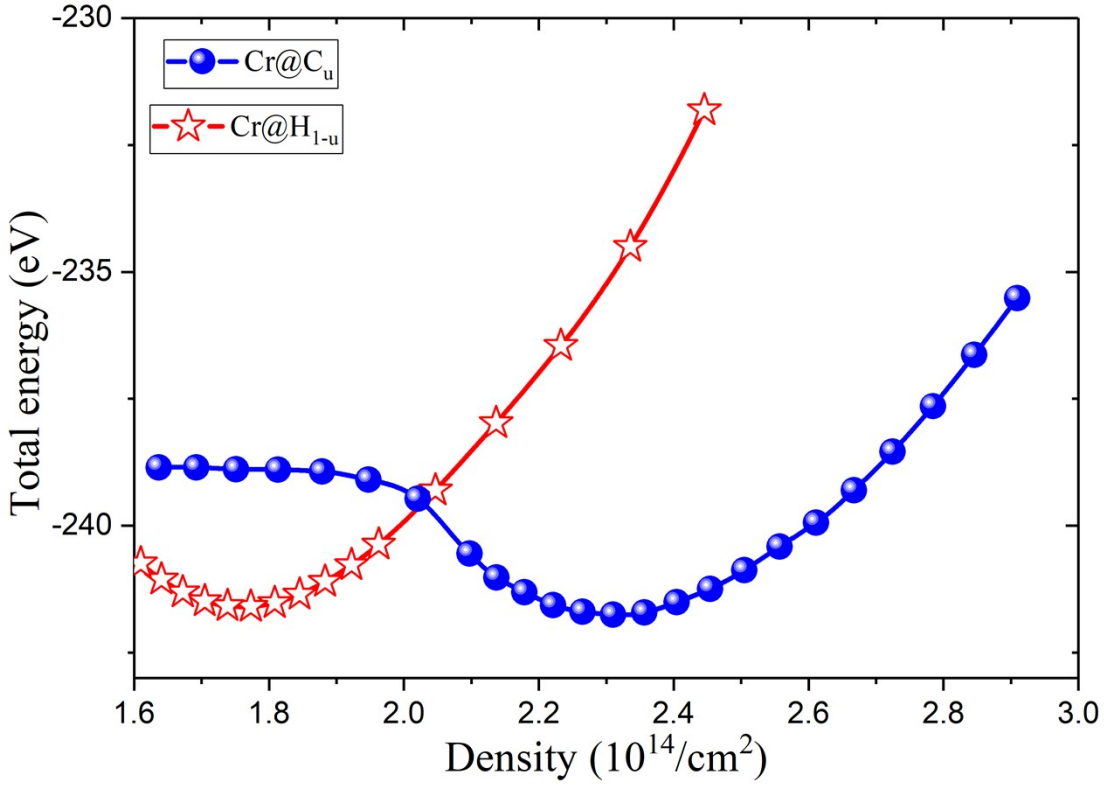

Fig. S2. Total energies of Cr@C_u and Cr@H_{1-u} versus the deposition density.

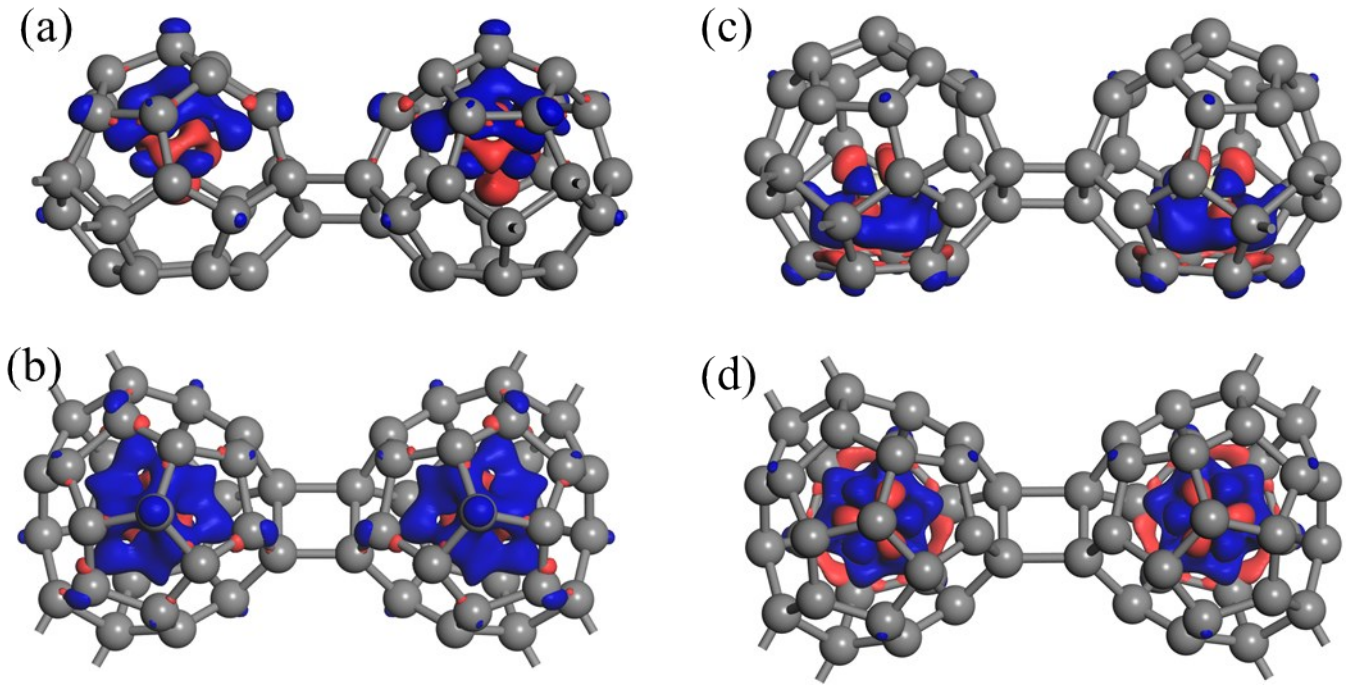

Fig. S3 (a) and (b) The side and top views of the charge redistribution of $Cr@H_{1\text{-}u}$. (c) and (d) The side and top views of the charge redistribution of $Cr@H_{1\text{-}d}$. (Red and blue colors indicate charge depletion and accumulation, the isosurface is $2.0\times10^{-3}e/Å^3$).

Table S5. The exchange energies of M@C, M@H_1 and M@H_2 (M= V-Zn).

	$V@C_u$	$V@C_d$	$V@H_{1\text{-}d}$	$V@H_{2\text{-}d}$	$Cr@C_u$	$Cr@C_d$	$Cr@H_{1\text{-}u}$	$Cr@H_{1\text{-}d}$
J_1 (meV)	3.38	2.44	1.13	1.11	0.07	0.06	0.32	1.08
	$Cr@H_{2\text{-}u}$	$Mn@C_u$	$Mn@C_d$	$Fe@H_{1\text{-}d}$	$Fe@H_{2\text{-}d}$	$Co@C_d$	$Ni@C_u$	$Ni@C_d$
J_1 (meV)	3.38	1.28	1.53	5.76	0.108	0.21	0.35	3.19
	$Cu@C_u$	$Cu@H_{2\text{-}u}$	$Zn@C_u$					
J_1 (meV)	1.12	1.18	1.33					

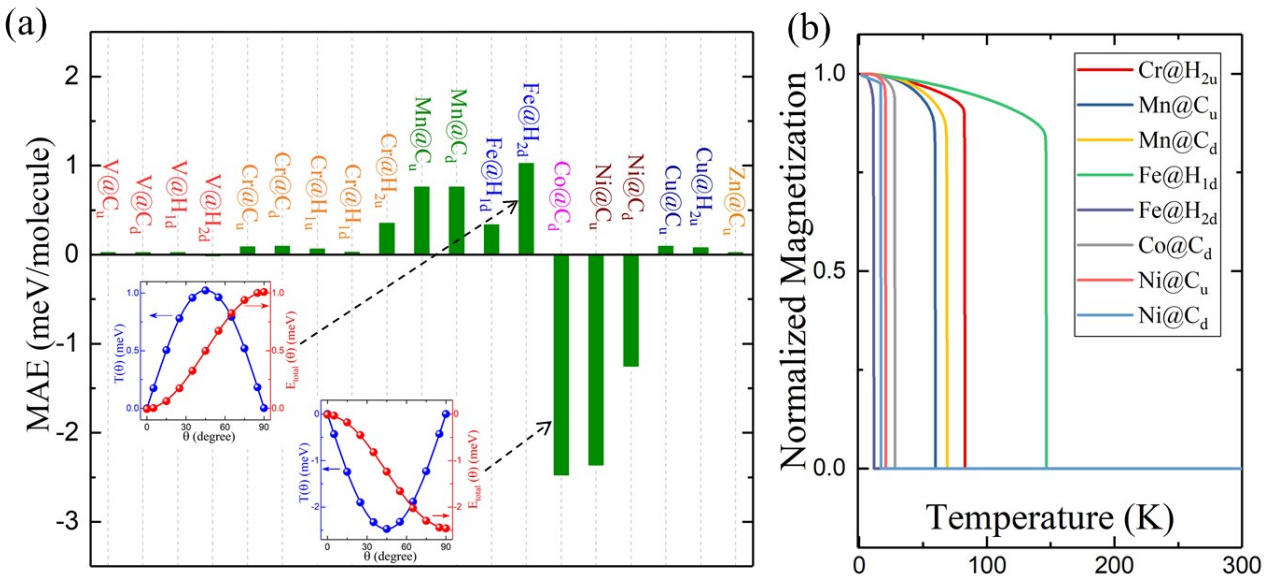

Fig. S4 (a) and (b) The calculated MAEs and the renormalized magnetization as a function of temperature T for some 2D covalent crystals with ferromagnetic ordering.

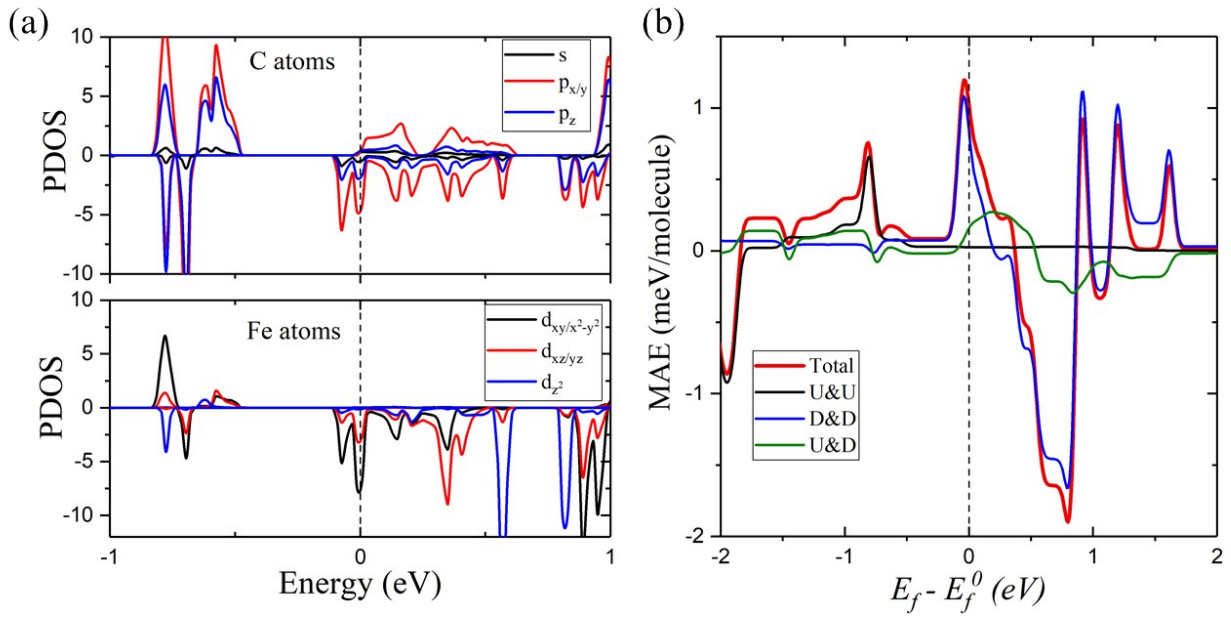

Fig. S5 (a) and (b) The projected density of states (PDOS) and the Fermi level dependent total and spin channel decomposed MAEs of Fe@$H_{2\text{-}d}$, respectively. One may see that the large perpendicular MAEs mostly stem from the SOC interaction between $d_{xy/(x^2-y^2)\downarrow}$ and $d_{xz/yz\downarrow}$ orbitals of Fe atom, and the cross-spin SOC interaction between $p_{x/y\uparrow}$ and $p_{x/y\downarrow}$ orbitals of the carbon cage also contributes. The total MAE is rather sensitive to the shift of the Fermi level, indicating a noteworthy magnetoelectric effect for this system, i.e., the MAEs can be effectively tuned by adjusting the position of the Fermi level.

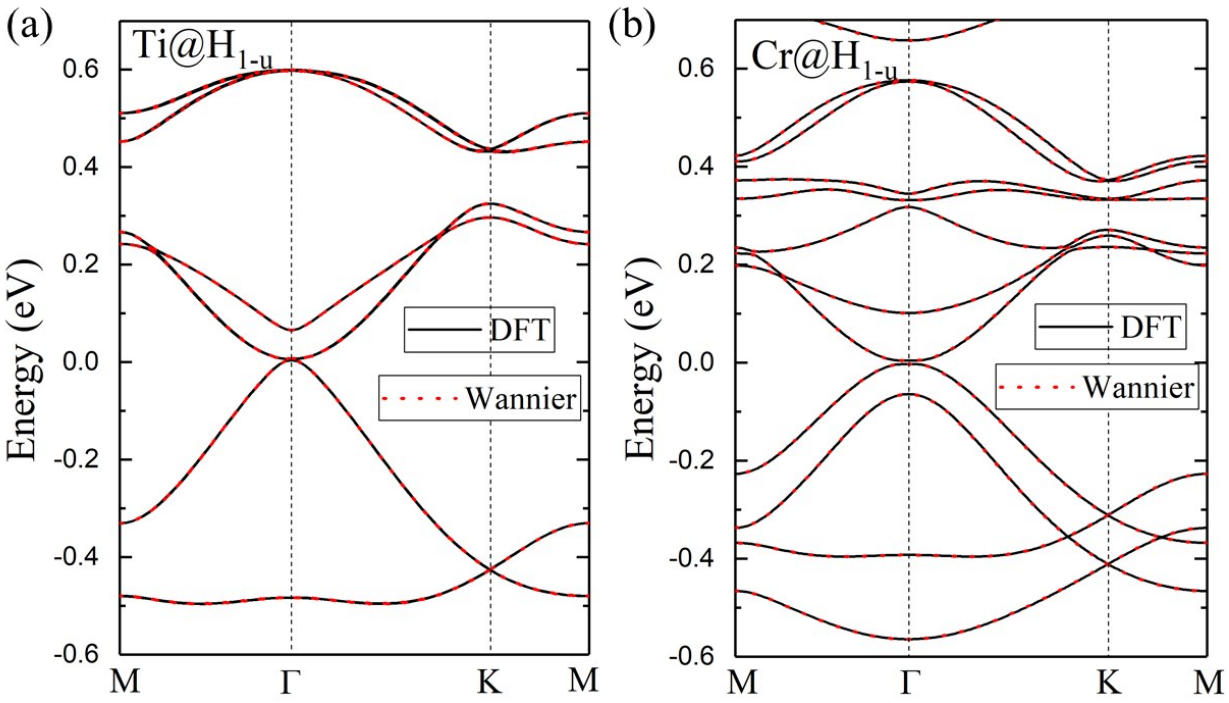

Fig. S6 (a) and (b) The band structures of $Ti@H_{1-u}$ and $Cr@H_{1-u}$ from DFT calculations and the fitting band structures by using the Wannier90 package, respectively.

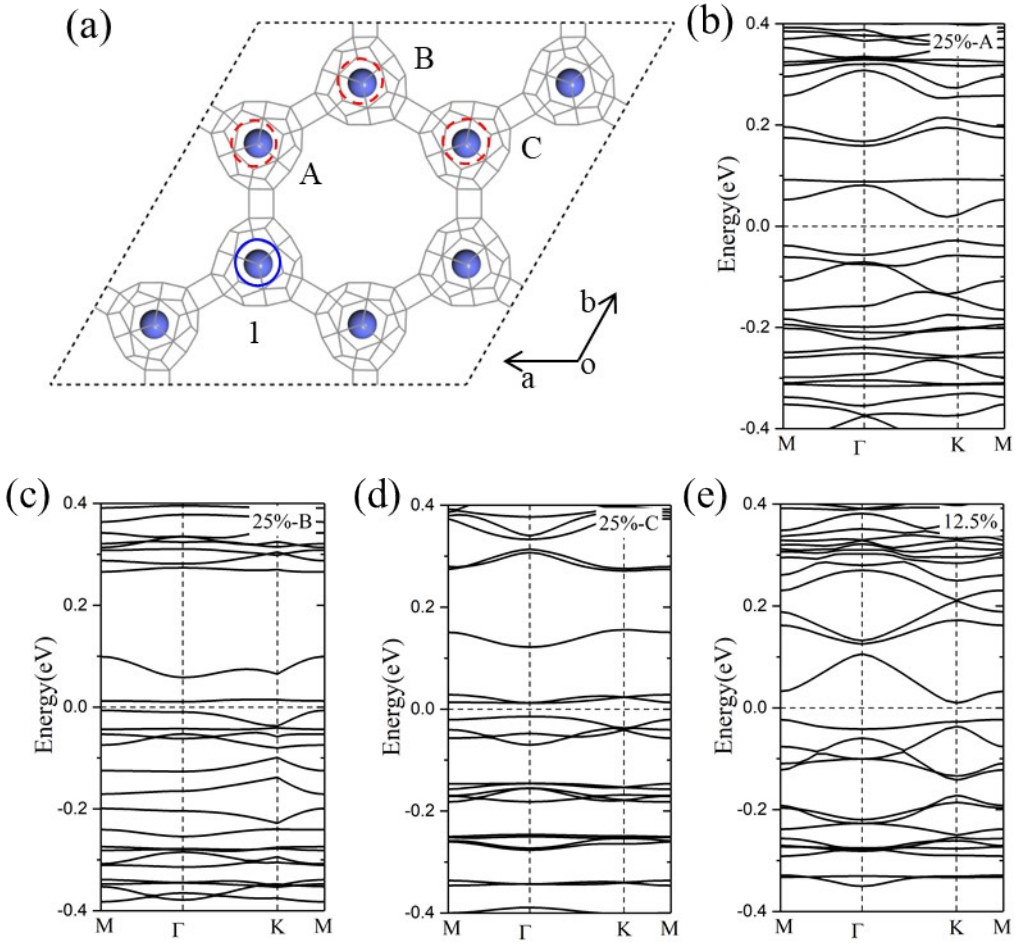

Fig. S7 (a) Schematic phase transition of the of $Cr@H_{1-u}$ lattice with two $Cr@C_{28}$ molecules being converted to phase II (25%), one is at site 1 and the other randomly takes site A, B or C. (b)-(d) Their corresponding band structures. (e) The band structure of $Cr@H_{1-u}$ with only one $Cr@C_{28}$ molecule in the supercell being converted to phase II (12.5%).